THE JOURNAL OF PHYSICAL CHEMISTRY Letters

Letter

pubs.acs.org/JPCL

Ultrahigh Vacuum Tip-Enhanced Raman Spectroscopy with Picosecond Excitation

Eric A. Pozzi,[†] Matthew D. Sonntag,[†] Nan Jiang,[†] Naihao Chiang,[§] Tamar Seideman,[†,§] Mark C. Hersam,[†,‡] and Richard P. Van Duyne*[,†,§]

[†]Department of Chemistry, [‡]Department of Materials Science and Engineering, and [§]Applied Physics Program, Northwestern University, Evanston, Illinois 60208, United States

Supporting Information

ABSTRACT: Tip-enhanced Raman spectroscopy (TERS) provides chemical information about adsorbates with nanoscale spatial resolution, but developments are still required in order to incorporate ultrafast temporal resolution. In this Letter, we demonstrate that a reliable TER signal of rhodamine 6G (R6G) using picosecond (ps)-pulsed excitation can be obtained in ultrahigh vacuum (UHV). In contrast to our previous observation of irreversible signal loss in ambient TERS (Klingsporn, J. M.; Sonntag, M. D.; Seideman, T.; Van Duyne, R. P. *J. Phys. Chem. Lett.* **2014**, *5*, 106−110), we demonstrate that the UHV environment decreases irreversible signal degradation. As a complement to the TERS experiments, we examined the rate of surface-enhanced Raman (SER) signal decay under picosecond irradiation and found that it is also slowed in UHV compared to that in ambient. Signal decay kinetics suggest that the predominant mechanism responsible for signal loss in ps SERS of R6G is surface diffusion. Both diffusive and reactive phenomena can lead to pulsed excitation TER signal loss, and a UHV environment is advantageous in either scenario.

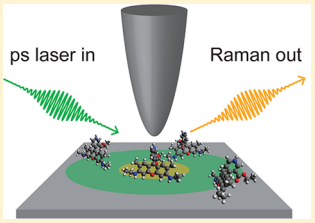

SECTION: Spectroscopy, Photochemistry, and Excited States

Ultrafast dynamics of molecules on surfaces are of fundamental importance to numerous fields, including solar energy, molecular electronics, and heterogeneous catalysis.[1,2] Techniques such as surface-enhanced femtosecond stimulated Raman spectroscopy (SE-FSRS),[3,4] surface-enhanced coherent anti-Stokes Raman spectroscopy (SE-CARS),[5,6] and time-resolved sum frequency generation (TR-SFG)[7−9] can probe the ultrafast dynamics of molecules on surfaces, but they do not intrinsically possess spatial resolution beyond the optical diffraction limit. In contrast, tip-enhanced Raman spectroscopy (TERS) has become an established tool capable of obtaining the vibrational spectra of adsorbates with nanoscale spatial resolution.[10−14] Coupled with scanning tunneling microscopy (STM) or atomic force microscopy (AFM), TERS can be utilized to gather correlated chemical and topographic information. TERS studies on atomically clean surfaces are possible when carried out in ultrahigh vacuum (UHV).[10,15−17] The spatial resolution of UHV-TERS was initially reported to be 15 nm.[18] Recently, spatial resolution of ∼1 nm has been reported in UHV[10] and ∼2 nm in ambient.[13] However, relatively few efforts to date have concentrated on incorporating ultrafast spectroscopic techniques with TERS. As a first step toward pump−probe TERS studies, efficient and reliable spontaneous TERS with pulsed excitation must be achieved.

Several groups have demonstrated advances in the area of temporally resolved TERS. The Kawata group reported tip-enhanced CARS of a DNA network.[19] The signal was not observed to degrade, demonstrating that the tip, surface, and molecules were able to withstand the high field intensities during the laser pulses. Wickramasinghe et al. demonstrated stimulated TERS (sTERS) of a thiol monolayer on Au(111).[20] In this study, the authors created a sTER image of the functionalized surface, and the Raman image more clearly reported the distribution of molecules than the images produced with concurrent STM. However, because only one Raman mode was stimulated in this study, the chemical information content of this work was limited. The Van Duyne group recently performed picosecond (ps) TERS of resonant species in ambient.[21] Multimodal TER spectra were collected in this work, but the signal was observed to diminish over the course of tens of seconds due to reactive decay chemistry of the resonant molecules. The authors suggested that performing pulsed excitation TERS on an atomically clean surface in UHV would be an effective way to prevent excited resonant analytes from reacting with small molecules present in ambient.

In this Letter, we present the successful coupling of picosecond-pulsed irradiation from an optical parametric oscillator (OPO) with our UHV-TERS instrument. Rhodamine 6G (R6G) was selected as the analyte due to its large resonant Raman cross section and compatibility with in situ sublimation.[16] We demonstrate that ps UHV-TERS of a resonant adsorbate can be observed without the permanent loss of signal that plagues ps TERS in ambient. Additionally, we investigate the mechanism responsible for R6G near-field signal decay under picosecond irradiation using surface-enhanced

Received: June 17, 2014
Accepted: July 21, 2014

   dx.doi.org/10.1021/jz501239z | *J. Phys. Chem. Lett.* 2014, 5, 2657−2661

Raman spectroscopy (SERS) and demonstrate that ps SERS signal loss can also be minimized in UHV.

We have reliably obtained the UHV-TER signal of R6G on Ag(111) using picosecond excitation. Figure 1A displays a time series of ps UHV-TER spectra obtained. The sample was exposed to constant irradiation throughout the acquisition. An electrochemically etched Ag STM tip was initially retracted from the surface and was brought into tunneling range at t = 60 s for the remainder of the acquisition. The R6G signal is absent with the tip retracted but becomes apparent upon engaging the tip. The signal-to-noise ratio (SNR) is predominantly above 3 with the tip engaged (Figure S1, Supporting Information), and, unlike the results previously obtained in ambient,[21] the signal is not irreversibly lost over time.

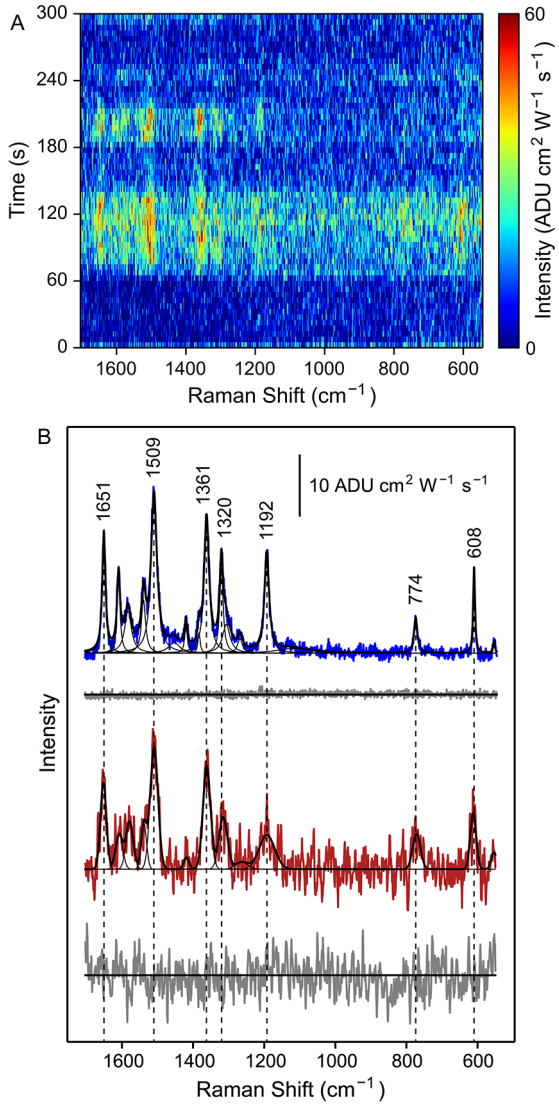

Figure 1. (A) Waterfall plot of sixty 5 s TER spectra of R6G collected using ps irradiation (λ = 532 nm, P_{ex} = 0.05 W/cm^2). The initially retracted Ag tip was brought into tunneling range at t = 60 s. (B) CW TER engaged (blue) and retracted (gray) spectra (λ = 532 nm, P_{ex} = 1.3 W/cm^2, t_{acq} = 30 s) plotted above averages of 12 ps TER engaged spectra with SNRs above 12 (red) and 12 retracted spectra (gray) from (A). Black lines represent individual and composite peak fits. The included scale bar applies to all plotted spectra.

In Figure 1B, UHV-TER near- and far-field spectra of R6G taken using continuous-wave (CW) excitation and the same Ag tip are plotted above averaged ps UHV-TER spectra from Figure 1A. Fits to the near-field data collected with both excitation sources unambiguously reveal the multimodal vibrational fingerprint of R6G.[16] A lower average laser power was used in ps UHV-TERS to limit the peak power during each laser pulse. As a result, the SNR is lower in the picosecond spectra.

While no permanent loss in ps UHV-TER signal is evident, large-amplitude intensity fluctuations are evident. In Figure 2A, a second ps UHV-TERS time series is presented, demonstrating the reproducibility of the near-field R6G signal, the lack of far-field R6G signal, and the existence of signal fluctuations. A third time series, depicted in Figure S2 (Supporting Information), exhibits similar features. This behavior is also observed using CW excitation (Figure 2B). Indeed, CW UHV-TERS fluctuations in both absolute and relative peak intensities are apparent, similar to results previously reported.[22] These observations are not surprising, considering the small number of molecules probed in TERS. Molecular diffusion is expected to cause the number of molecules in the enhancing region to vary over time. This conclusion is in line with UHV STM imaging of R6G/Ag(111), which exhibits streaks in the scan direction, indicating that R6G diffuses on the Ag surface at room temperature (Figure S3, Supporting Information). Another possible explanation for the observed signal fluctua-

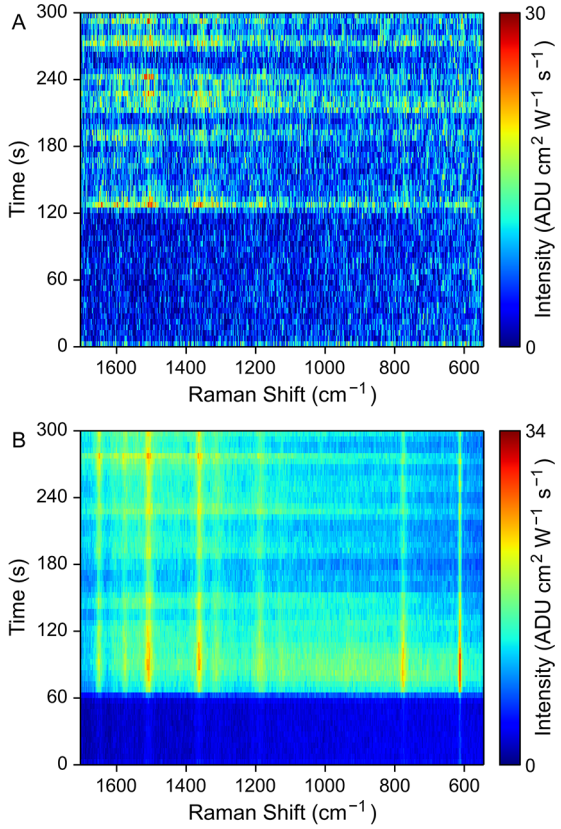

Figure 2. Waterfall plots of sixty 5 s TER spectra of R6G collected using (A) ps irradiation (λ = 532 nm, P_{ex} = 0.13 W/cm^2) and (B) CW irradiation (λ = 532 nm, P_{ex} = 1.3 W/cm^2). The Ag tip was brought into tunneling range at t = 120 and 60 s for (A) and (B), respectively.

dx.doi.org/10.1021/jz501239z | J. Phys. Chem. Lett. 2014, 5, 2657−2661

tions may lie in thermal fluctuations at the tip−sample junction.[17]

Fluctuations and a low SNR in ps UHV-TERS complicate quantitative analysis of the signal's temporal response. In contrast, SERS sums contributions from many electromagnetic hot spots and overcomes both of these issues. To investigate the influence of the UHV environment on near-field signal permanence, we collected ps SERS time series from the same sample in UHV and in ambient. A Ag film over nanospheres (AgFON) substrate[23] was degassed in UHV to remove any volatile contaminants prior to R6G sublimation and subsequent spectroscopy. Following ps UHV-SERS collection, the sample was removed from UHV, after which ambient ps SERS was acquired using irradiation of equivalent power density. Signal intensities were calculated by integrating the intensities of major R6G peaks (610, 1192, 1361, 1509, and 1651 cm^{-1}), and peak intensities from two representative peaks are plotted as functions of time in Figure 3. Decreases in the SERS signal over

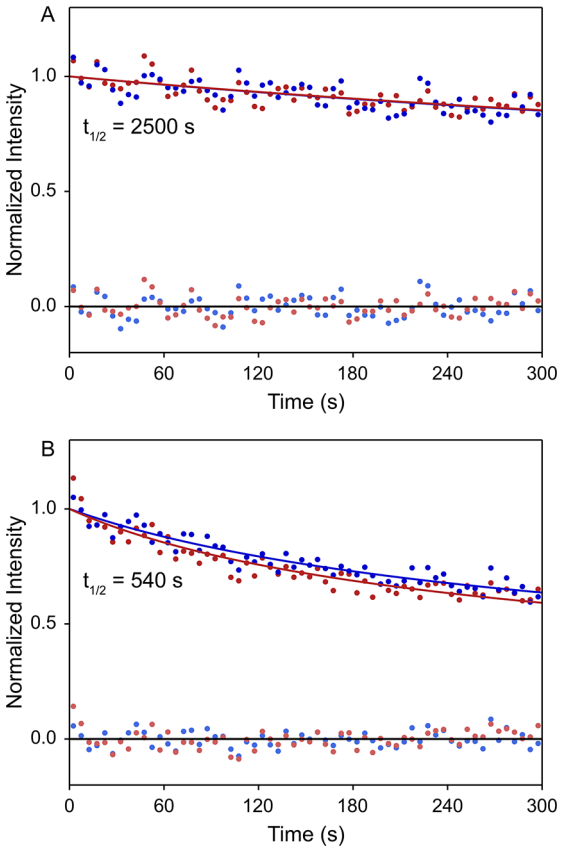

Figure 3. Integrated intensities of the 1361 (red) and 1509 cm^{-1} (blue) peaks of R6G as a function of time for 1.3 W/cm^2 (A) ps UHV-SERS and (B) ps ambient SERS (t_{acq} = 5 s, 60 spectra). Data (dots) for each peak are fitted with $t^{-1/2}$ curves (solid lines), and fit residuals are plotted about the horizontal axes.

time were observed in both cases, with the effect more pronounced in ambient. By modeling the decay using diffusion kinetics (see below), the signal half-life in UHV was calculated to be 2500 s compared to 540 s in ambient. The ∼5× greater signal stability in UHV will allow for longer averaging times during ultrafast pump−probe experiments. The ps SERS time series, from which the integrated intensities were calculated, are displayed in Figure S4 (Supporting Information).

Ambient SERS was also performed at orders of magnitude higher power density to exaggerate signal decay and to characterize its shape (Figure 4). Intensities were calculated

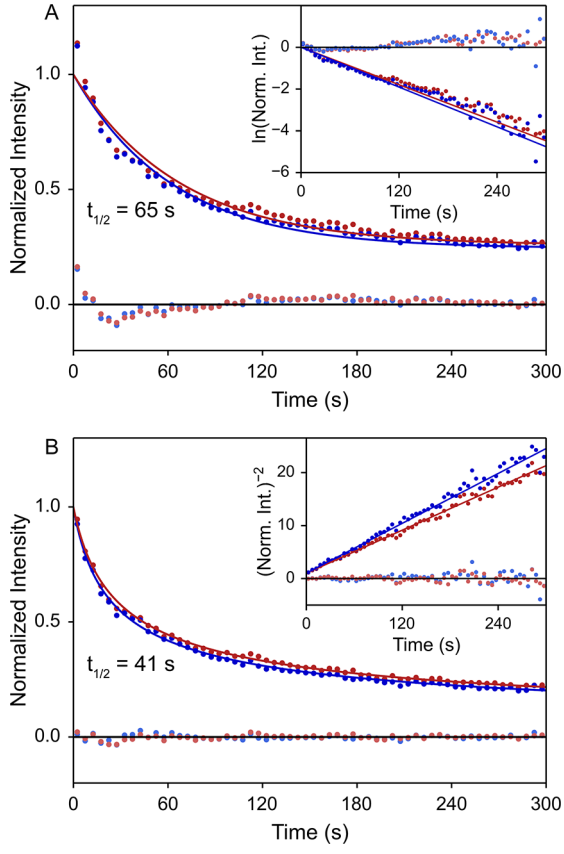

Figure 4. Integrated intensities of the 1361 (red) and 1509 cm^{-1} (blue) peaks of R6G as a function of time for 130 W/cm^2 ps ambient SERS (t_{acq} = 5 s, 60 spectra). Data (dots) for each peak are fitted with (A) $e^{-t/\tau}$ and (B) $t^{-1/2}$ curves (solid lines), and fit residuals are plotted about the horizontal axes. The insets depict linearized plots for each kinetic model.

by integrating the areas under the major peaks mentioned above. Kinetic models for reactive decay chemistry and for diffusion were utilized to probe the underlying mechanism for the observed signal loss. The deviation from linearity observed in the plot of ln(intensity) versus time suggests that reactive decay is not the main source of signal loss. In contrast, due to the linear nature of the intensity^{-2} versus time plot, diffusion appears to be the dominant mechanism responsible.

Previous reports indicate that a water meniscus several nanometers thick exists on high surface energy substrates in ambient,[24,25] through which molecules are able to diffuse. In 10^{-11} Torr UHV, the water meniscus on the AgFON should be minimized or eliminated after degassing, resulting in slower surface diffusion rates. Signal loss due to diffusion suggests that the picosecond pulses heat SERS hot spots. It follows that the faster signal decay at higher laser power is the result of greater heating. Knowledge of local surface temperatures is then required in order to extract diffusion coefficients of R6G in both environments. At present, the laser power losses due to fiber coupling and grating filtration in our apparatus prevented the collection of ps UHV-SERS at higher power density.

Applying this knowledge to ps TERS requires the acknowledgment of inherent differences between the two techniques.

dx.doi.org/10.1021/jz501239z | J. Phys. Chem. Lett. 2014, 5, 2657−2661

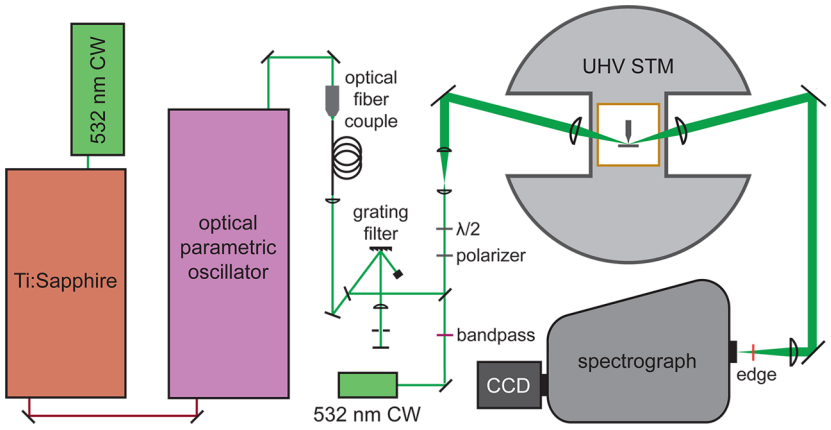

Figure 5. The ps UHV-TERS experimental schematic. Pulsed 532 nm irradiation is coupled to the UHV instrument via an optical fiber, after which it is cleaned in the frequency domain with a grating filter and aligned collinear with a 532 nm CW beam.

First, the surface of a AgFON is rough on the ∼100 nm length scale, whereas the Ag(111) surface is not. Consequently, the diffusion kinetics are expected to be altered and perhaps slowed on the AgFON versus those on Ag(111). Next, diffusion in SERS occurs from many point sources as opposed to one point source in TERS. A molecule diffusing from a particular SERS hot spot will then approach another hot spot; this phenomenon is likely to slow signal decay in SERS. In addition, whereas the Ag(111) surface is atomically clean due to complete in vacuo preparation, the AgFON prepared external to the chamber and brought into the UHV environment is not. Although the AgFON is degassed overnight, we cannot be certain that the water meniscus is completely removed.

Taking into account previous results[21] indicating that reactive decay chemistry can be responsible for signal decay for certain ps TERS systems, it is clear that both reaction and diffusion can cause signal loss during pulsed excitation, plasmonically enhanced experiments. Reactive decay chemistry evidently dominates for chemisorbed species, for example, malachite green isothiocyanate (MGITC),[21] while diffusive behavior provides another mechanism for signal loss of physisorbed species. Importantly, a UHV environment minimizes ps TER signal loss from both diffusive and reactive sources. Specifically, the lack of a water meniscus in UHV-TERS slows diffusion as molecules are restricted to motion in two dimensions. In addition, elimination of small molecules, such as water and oxygen, blocks reactive decay pathways.

In conclusion, we have demonstrated ps UHV-TERS of the R6G/Ag(111) system. The signal intensity is observed to fluctuate over time in a manner that is comparable to CW UHV-TERS. This phenomenon is likely a result of R6G surface diffusion, which causes the number of molecules in the hot spot, and thus the TER signal intensity, to vary over time. While the fluctuations and a low SNR prevent rigorous characterization of signal intensity versus time, it is clear that the signal is not irreversibly lost. The ps SERS experiments suggest that diffusion is the dominant mechanism responsible for R6G signal decay and that this effect is minimized in UHV. While the exact decay mechanism in ps TERS for a particular surface−adsorbate system may be diffusion and/or reactive decay chemistry, the UHV environment suppresses both mechanisms, improving measurement stability. A UHV environment for temporally resolved TERS experiments is thus a valuable asset for studying the spatially resolved dynamics of surface-bound molecules.

EXPERIMENTAL METHODS

A schematic of the optical setup used in this study is depicted in Figure 5. Picosecond (ps) pulses were generated by a laser system tunable from 500 to 1600 nm.[21] Briefly, A CW 532 nm diode-pumped solid-state laser (Spectra-Physics Millenia XV) and a Ti:sapphire mode-locked laser (Spectra Physics Tsunami) pumped a synchronously pumped intracavity doubled optical parametric oscillator (Coherent Mira-OPO). Pulses on the order of 1 ps in length were produced at a repetition rate of 80 MHz. The OPO output was tuned to 532 nm and fiber-optically launched through a single-mode fiber to the UHV STM. The Raman background generated in the fiber was removed by spectrally dispersing the beam using a grating filter (Thorlabs 1800 gr/mm). The picosecond beam was then inserted into the beam path of the 532 nm CW laser (Spectra-Physics Excelsior).

UHV-TERS and -SERS were performed using the same instrument as that described previously, with a base pressure of ∼2×10^{-11} Torr.[15,16] The laser excitation polarization was rotated using a half-wave plate to be p-polarized with respect to the tip axis. The beam was then expanded before a 50 mm (focal length, 100 mm) lens focused the light on the tip−sample junction at an angle of roughly 75° with respect to the Ag(111) normal. An identical lens collimated the collection light, which was then focused on the entrance slit of an imaging spectrograph (Princeton Instruments SCT 320) and detected by a thermoelectrically cooled charge coupled device (CCD) (Princeton Instruments Pixis 400). TER spectra were acquired using a sample bias of +1 V with respect to the grounded tip, and the tunneling current set point was 100 pA.

Electrochemically etched Ag tips[15,26] were brought into UHV immediately after fabrication and used without further treatment. The Ag(111) sample was prepared in UHV via cycles of Ar^+ sputtering and thermal annealing, and R6G molecules were deposited via sublimation.[16] The AgFON substrate was fabricated by drop-casting 390 nm silica spheres onto a Si wafer and thermally evaporating a 200 nm Ag layer onto the sphere mask.[23,27] The substrate was designed to exhibit optimal enhancement for 532 nm excitation.[27] The AgFON was brought into UHV immediately after fabrication and degassed at ∼105 °C overnight before R6G sublimation.

After UHV-SERS was performed, the same AgFON sample was then removed from UHV in order to perform ambient SERS using an inverted microscope. A 20× extra-long working

dx.doi.org/10.1021/jz501239z | J. Phys. Chem. Lett. 2014, 5, 2657−2661

distance objective focused the picosecond beam onto the substrate and collected the SER-scattered light, which was then focused on the entrance slit of the single-stage spectrograph (Princeton Instruments Acton SpectraPro 2300i) and detected using a liquid-N_2-cooled CCD (Princeton Instruments Spec-10:400BR).

■ ASSOCIATED CONTENT

Supporting Information

The ps UHV-TERS integrated intensity versus time plots, an additional ps UHV-TERS waterfall plot, UHV STM image of R6G on Ag(111), and ps SERS waterfall plots in UHV and in ambient. This material is available free of charge via the Internet at http://pubs.acs.org.

■ AUTHOR INFORMATION

Corresponding Author

*E-mail: vanduyne@northwestern.edu.

Notes

The authors declare no competing financial interest.

■ ACKNOWLEDGMENTS

This work was supported by the Department of Energy Office of Basic Energy Sciences (DE-FG02-09ER16109) and the Air Force Office of Scientific Research Multidisciplinary University Research Initiative (FA9550-14-1-003). Additional support was provided by the National Science Foundation (DMR-1121262) and the National Science Foundation Center for Chemical Innovation dedicated to Chemistry at the Space−Time Limit (CHE-082913). This material is based upon work supported by the National Science Foundation Graduate Research Fellowship under Grant No. DGE-1324585. Any opinions, findings, and conclusions or recommendations expressed in this material are those of the authors and do not necessarily reflect the views of the National Science Foundation.

■ REFERENCES

(1) Barbara, P. F.; Meyer, T. J.; Ratner, M. A. Contemporary Issues in Electron Transfer Research. *J. Phys. Chem.* **1996**, *100*, 13148−13168.
(2) Zewail, A. H. Femtochemistry: Atomic-Scale Dynamics of the Chemical Bond. *J. Phys. Chem. A* **2000**, *104*, 5660−5694.
(3) Frontiera, R. R.; Henry, A.-I.; Gruenke, N. L.; Van Duyne, R. P. Surface-Enhanced Femtosecond Stimulated Raman Spectroscopy. *J. Phys. Chem. Lett.* **2011**, *2*, 1199−1203.
(4) Frontiera, R. R.; Gruenke, N. L.; Van Duyne, R. P. Fano-Like Resonances Arising from Long-Lived Molecule−Plasmon Interactions in Colloidal Nanoantennas. *Nano Lett.* **2012**, *12*, 5989−5994.
(5) Steuwe, C.; Kaminski, C. F.; Baumberg, J. J.; Mahajan, S. Surface Enhanced Coherent Anti-Stokes Raman Scattering on Nanostructured Gold Surfaces. *Nano Lett.* **2011**, *11*, 5339−5343.
(6) Ideguchi, T.; Holzner, S.; Bernhardt, B.; Guelachvili, G.; Picque, N.; Hansch, T. W. Coherent Raman Spectro-Imaging with Laser Frequency Combs. *Nature* **2013**, *502*, 355−358.
(7) Bordenyuk, A. N.; Benderskii, A. V. Spectrally- and Time-Resolved Vibrational Surface Spectroscopy: Ultrafast Hydrogen-Bonding Dynamics at D_2O/CaF_2 Interface. *J. Chem. Phys.* **2005**, *122*, 134713.
(8) Berg, C. M.; Lagutchev, A.; Dlott, D. D. Probing of Molecular Adsorbates on Au Surfaces with Large-Amplitude Temperature Jumps. *J. Appl. Phys.* **2013**, *113*, 183509.
(9) Laaser, J. E.; Skoff, D. R.; Ho, J. J.; Joo, Y.; Serrano, A. L.; Steinkruger, J. D.; Gopalan, P.; Gellman, S. H.; Zanni, M. T. Two-Dimensional Sum-Frequency Generation Reveals Structure and Dynamics of a Surface-Bound Peptide. *J. Am. Chem. Soc.* **2014**, *136*, 956−962.
(10) Zhang, R.; Zhang, Y.; Dong, Z. C.; Jiang, S.; Zhang, C.; Chen, L. G.; Zhang, L.; Liao, Y.; Aizpurua, J.; Luo, Y.; Yang, J. L.; Hou, J. G. Chemical Mapping of a Single Molecule by Plasmon-Enhanced Raman Scattering. *Nature* **2013**, *498*, 82−86.
(11) Schmid, T.; Opilik, L.; Blum, C.; Zenobi, R. Nanoscale Chemical Imaging Using Tip-Enhanced Raman Spectroscopy: A Critical Review. *Angew. Chem., Int. Ed.* **2013**, *52*, 5940−5954.
(12) Pozzi, E. A.; Sonntag, M. D.; Jiang, N.; Klingsporn, J. M.; Hersam, M. C.; Van Duyne, R. P. Tip-Enhanced Raman Imaging: An Emergent Tool for Probing Biology at the Nanoscale. *ACS Nano* **2013**, *7*, 885−888.
(13) Chen, C.; Hayazawa, N.; Kawata, S. A 1.7 nm Resolution Chemical Analysis of Carbon Nanotubes by Tip-Enhanced Raman Imaging in the Ambient. *Nat. Commun.* **2014**, *5*, 3312.
(14) Sonntag, M. D.; Klingsporn, J. M.; Zrimsek, A. B.; Sharma, B.; Ruvuna, L. K.; Van Duyne, R. P. Molecular Plasmonics for Nanoscale Spectroscopy. *Chem. Soc. Rev.* **2014**, *43*, 1230−1247.
(15) Jiang, N.; Foley, E. T.; Klingsporn, J. M.; Sonntag, M. D.; Valley, N. A.; Dieringer, J. A.; Seideman, T.; Schatz, G. C.; Hersam, M. C.; Van Duyne, R. P. Observation of Multiple Vibrational Modes in Ultrahigh Vacuum Tip-Enhanced Raman Spectroscopy Combined with Molecular-Resolution Scanning Tunneling Microscopy. *Nano Lett.* **2012**, *12*, 5061−5067.
(16) Klingsporn, J. M.; Jiang, N.; Pozzi, E. A.; Sonntag, M. D.; Chulhai, D.; Seideman, T.; Jensen, L.; Hersam, M. C.; Van Duyne, R. P. Intramolecular Insight into Adsorbate−Substrate Interactions via Low-Temperature, Ultrahigh-Vacuum Tip-Enhanced Raman Spectroscopy. *J. Am. Chem. Soc.* **2014**, *136*, 3881−3887.
(17) Shiotari, A.; Kumagai, T.; Wolf, M. Tip-Enhanced Raman Spectroscopy of Graphene Nanoribbons on Au(111). *J. Phys. Chem. C* **2014**, *118*, 11806−11812.
(18) Steidtner, J.; Pettinger, B. Tip-Enhanced Raman Spectroscopy and Microscopy on Single Dye Molecules with 15 nm Resolution. *Phys. Rev. Lett.* **2008**, *100*, 236101.
(19) Ichimura, T.; Hayazawa, N.; Hashimoto, M.; Inouye, Y.; Kawata, S. Tip-Enhanced Coherent Anti-Stokes Raman Scattering for Vibrational Nanoimaging. *Phys. Rev. Lett.* **2004**, *92*, 220801.
(20) Wickramasinghe, H. K.; Chaigneau, M.; Yasukuni, R.; Picardi, G.; Ossikovski, R. Billion-Fold Increase in Tip-Enhanced Raman Signal. *ACS Nano* **2014**, *8*, 3421−3426.
(21) Klingsporn, J. M.; Sonntag, M. D.; Seideman, T.; Van Duyne, R. P. Tip-Enhanced Raman Spectroscopy with Picosecond Pulses. *J. Phys. Chem. Lett.* **2014**, *5*, 106−110.
(22) Sonntag, M. D.; Chulhai, D.; Seideman, T.; Jensen, L.; Van Duyne, R. P. The Origin of Relative Intensity Fluctuations in Single-Molecule Tip-Enhanced Raman Spectroscopy. *J. Am. Chem. Soc.* **2013**, *135*, 17187−17192.
(23) Hulteen, J. C.; Treichel, D. A.; Smith, M. T.; Duval, M. L.; Jensen, T. R.; Van Duyne, R. P. Nanosphere Lithography: Size-Tunable Silver Nanoparticle and Surface Cluster Arrays. *J. Phys. Chem. B* **1999**, *103*, 3854−3863.
(24) Cappella, B.; Dietler, G. Force−Distance Curves by Atomic Force Microscopy. *Surf. Sci. Rep.* **1999**, *34*, 1−104.
(25) Weeks, B. L.; Vaughn, M. W.; DeYoreo, J. J. Direct Imaging of Meniscus Formation in Atomic Force Microscopy Using Environmental Scanning Electron Microscopy. *Langmuir* **2005**, *21*, 8096−8098.
(26) Iwami, M.; Uehara, Y.; Ushioda, S. Preparation of Silver Tips for Scanning Tunneling Microscopy Imaging. *Rev. Sci. Instrum.* **1998**, *69*, 4010−4011.
(27) Greeneltch, N. G.; Blaber, M. G.; Henry, A. I.; Schatz, G. C.; Van Duyne, R. P. Immobilized Nanorod Assemblies: Fabrication and Understanding of Large Area Surface-Enhanced Raman Spectroscopy Substrates. *Anal. Chem.* **2013**, *85*, 2297−2303.